

REFERENCES

Technical Books

- Beer, F. P., and Johnston, E. R., 1988, *Vector Mechanics for Engineers – Statics*, McGraw-Hill, Inc., New York, pp. 14-32.
- Blake, A., 1986, *Threaded Fasteners*, Marcel Dekker Inc., New York, pp. 7-26.
- Craig, John J., 1989, *Introduction to Robotics, Mechanics and Control*, Addison-Wesley, Inc., New York, pp. 19-60.
- Crane III, C. D., and Duffy, J., 1998, *Kinematic Analysis of Robot Manipulators*, Cambridge University Press, New York, pp. 4-36.
- Dimentberg, F. M., 1965, *The Screw Calculus and its Applications in Mechanics*, Foreign Technology Division, Wright-Patterson Air Force Base, Ohio. Document No. FTD-HT-23-1632-67.
- Hunt, K. H., 1978, *Kinematic Geometry of Mechanisms*, Oxford University Press, New York, pp. 304-374.
- Klafter, R. D., Chmielewski, T. A., and Negin, M., 1989, *Robotic Engineering An Integrated Approach*, Prentice Hall, Inc., New Jersey, pp. 561-661.
- McCrea, William H., 1947, *Analytical Geometry of Three Dimensions*, Interscience Publishers, Inc., New York, pp.41-53.
- Meirovitch, Leonard, 1970, *Methods of Analytical Dynamics*, McGraw-Hill, Inc., pp. 101-110.
- Munem, M. A., and Foulis, D. J., 1984, *Calculus with Analytical Geometry*, Worth Publishers, Inc., New York, pp. 709-826.
- Nevins, J. L., and Whitney, D. E., 1989, *Concurrent Design of Products and Processes: A Strategy for the Next Generation in Manufacturing*, McGraw-Hill, Inc., New York, pp. 116-120.
- Oberg, E., Jones, F. D., Horton, H. L., Ryffel, H. H., Green, R. E. ed., 1992, *Machinery's Handbook 24th Edition*, Industrial Press, Inc., New York, pp. 1520-1527.
- Semple, J. G., Roth, L., 1949, *Introduction to Algebraic Geometry*, Oxford University Press, New York, pp. 233-295.
- Wrede, Robert C., 1972, *Introduction to Vector and Tensor Analysis*, Dover Publications, Inc., pp. 96-122.

Theses

Caine, M. E., 1985, "Chamferless Assembly of Rectangular Parts in Two and Three Dimensions," Master Thesis, Massachusetts Institute of Technology, Dept. of Mechanical Engineering, June.

Ohwovoriole, M.S., 1980, "An Extension of Screw Theory and Its Application to the Automation of Industrial Assemblies," Ph.D. thesis, Stanford University Dept. of Computer Science, April.

Conference Proceedings

Gottschalk, S., Lin, M. C., and Manocha, D., 1996, "OBB-Tree: A Hierarchical Structure for Rapid Interference Detection," Technical report TR96-013, Department of Computer Science, University of N. Carolina, Chapel Hill.

Nicolson, E. J., and Fearing, R. S., 1991, "Dynamics Modeling of Part Mating Problem: Threaded Fastener Insertion," *Proc. IEEE/RSJ International Workshop on Intelligent Robots and Systems*, pp. 30-37.

Nicolson, E. J., and Fearing, R. S., 1993, "Compliant Control of Threaded Fastener Insertion," *National Science Foundation, IEEE*, pp. 484-490.

Sathirakul, K., and Sturges, R. H., 1998, "Compliance Design Through Constraint Network Analysis," *Proc. of the Japan-USA Symposium on Flexible Automation*, Otsu, Japan.

Strip, D., 1988, "Insertions Using Geometric Analysis and Hybrid Force-Position Control: Method and Analysis," *IEEE International Conference on Robotics and Automation*, Philadelphia, Pennsylvania, USA, pp. 1744-1751.

Qiao, H., Dalay, B. S., and Parkin, R. M., 1994, "Precise Robotic Chamferless Peg-Hole Insertion Operation Without Force Feedback and Remote Center Compliance (RCC)," *Proc. of the Institution of Mechanical Engineers*, Vol. 208, No. 2, pp. 89-104.

Journal Articles

Dhayagude, N., Gao, Z., Mrad, F., 1996, "Fuzzy Logic Control of Automated Screw Fastening," *Robotics & Computer Integrated Manufacturing*, Vol. 12, No. 3, pp. 235-242.

McCarragher, B. J., and Asada, H., 1995, "A Discrete Event Approach to the Control of Robotic Assembly Tasks," *ASME Journal of Dynamic Systems, Measurement, and Control*, Vol. 117, September, pp. 384-393.

Nevins, J. L., and Whitney, D. E., 1980, "Assembly Research," *Factory Automation*, Vol. 2, Maidenhead, England, pp. 26-44.

Sturges, R. H., and Laowattana, S., 1996, "Virtual Wedging in Three-Dimensional Peg Insertion Tasks," *ASME Journal of Mechanical Design*, Vol. 118, March, pp. 99-105.

Sturges, R. H., and Laowattana, S., 1996, "Design of an Orthogonal Compliance for Polygonal Peg Insertion," *ASME Journal of Mechanical Design*, Vol. 118, March, pp. 106-114.

Whitney, D. E., 1982, "Quasi-Static Assembly of Compliantly Supported Rigid Parts," *ASME Journal of Dynamic Systems, Measurement, and Control*, Vol. 104, March, pp. 65-77.

Whitney, D. E., and Rourke, J. M., 1986, "Mechanical Behavior and Design Equations for Elastomer Shear Pad Remote Center Compliances," *ASME Journal of Dynamic Systems, Measurement, and Control*, Vol. 108, September, pp. 223-232.

Russian Engineering Journal Articles

Andreev, G. Ya., and Laktionov, N. M., 1966, "Problems in the Assembly of Large Parts," *Russian Engineering Journal*, Vol. 46, No. 1, pp. 60-61.

Andreev, G. Ya., 1972, "Assembling Cylindrical Press-Fit Joints," *Russian Engineering Journal*, Vol. 52, No. 7, pp. 54-57.

Andreev, G. Ya., and Laktionov, N. M., 1969, "Contact Stresses During Automatic Assembly," *Russian Engineering Journal*, Vol. 49, No. 11, pp. 57-60.

Blaer, I. L., 1962, "Reliable Automatic Starting of Threaded Parts," *Russian Engineering Journal*, Vol. 42, No. 12, pp. 32-34.

Gusev, A. S., 1969, "Automatic Assembly of Cylindrically-Shaped Components," *Russian Engineering Journal*, Vol. 49, No. 11, pp. 53-57.

Karelin, M. M., and Girel, A. M., 1967, "The Accurate Alignment of Parts for Automatic Assembly," *Russian Engineering Journal*, Vol. 47, No. 9, pp. 73-76.

Laktionov, N. M., and Andreev, G. Ya., 1966, "The Automatic Assembly of Parts," *Russian Engineering Journal*, Vol. 46, No. 8, pp. 40-43.

Romanov, G. I., 1964, "Preventing Thread Shear in Automatic Assembly," *Russian Engineering Journal*, Vol. 44, No. 9, pp. 50-52.

Savishchenko, V. M., and Bepalov, V. G., 1965, "The Orientation of Components for Automatic Assembly," *Russian Engineering Journal*, Vol. 45, No. 5, pp. 50-52.

APPENDIX A

A.1 BOLT PARAMETRIC EQUATIONS

1. Positive Flank Radius

$$R_{+F} = (b_{\max} - \frac{1}{2}crr_b) - K(\theta + \theta_{ini})$$

$$0.0000 \leq \theta \leq 0.5959 \quad \theta_{ini} = 1.0955$$

$$\bar{\mathbf{P}} = R_{+F} \cos(\theta) \hat{\mathbf{i}} + R_{+F} \sin(\theta) \hat{\mathbf{j}}$$

$$\bar{\mathbf{T}} = \left\{ -K \cos(\theta) - \left[(b_{\max} - \frac{1}{2}crr_b) - K(\theta + \theta_{ini}) \right] \sin(\theta) \right\} \hat{\mathbf{i}}$$

$$\left\{ -K \sin(\theta) + \left[(b_{\max} - \frac{1}{2}crr_b) - K(\theta + \theta_{ini}) \right] \cos(\theta) \right\} \hat{\mathbf{j}}$$

2. Positive Root Fillet Radius

$$R_{+RF} = (b_{\min} + rr_b) - \sqrt{rr_b^2 - \left(\frac{\sqrt{3}}{2} rr_b - L(\theta - \theta_{ini}) \right)^2}$$

$$0.5959 < \theta \leq 1.1400 \quad \theta_{ini} = 0.5959$$

$$\bar{\mathbf{P}} = R_{+RF} \cos(\theta) \hat{\mathbf{i}} + R_{+RF} \sin(\theta) \hat{\mathbf{j}}$$

$$\bar{\mathbf{T}} = \left\{ \frac{-L \left(\frac{\sqrt{3}}{2} rr_b - L(\theta - \theta_{ini}) \right) \cos(\theta)}{\sqrt{rr_b^2 - \left(\frac{\sqrt{3}}{2} rr_b - L(\theta - \theta_{ini}) \right)^2}} - \left[(b_{\min} + rr_b) - \sqrt{rr_b^2 - \left(\frac{\sqrt{3}}{2} rr_b - L(\theta - \theta_{ini}) \right)^2} \right] \sin(\theta) \right\} \hat{\mathbf{i}}$$

$$\left\{ \frac{-L \left(\frac{\sqrt{3}}{2} rr_b - L(\theta - \theta_{ini}) \right) \sin(\theta)}{\sqrt{rr_b^2 - \left(\frac{\sqrt{3}}{2} rr_b - L(\theta - \theta_{ini}) \right)^2}} + \left[(b_{\min} + rr_b) - \sqrt{rr_b^2 - \left(\frac{\sqrt{3}}{2} rr_b - L(\theta - \theta_{ini}) \right)^2} \right] \cos(\theta) \right\} \hat{\mathbf{j}}$$

3. Root Radius

$$R_R = b_{\min}$$

$$1.14003 < \theta \leq 1.9853 \quad \theta_{ini} = 1.14003$$

$$\bar{\mathbf{P}} = b_{\min} \cos(\theta) \hat{\mathbf{i}} + b_{\min} \sin(\theta) \hat{\mathbf{j}}$$

$$\bar{\mathbf{T}} = -b_{\min} \sin(\theta) \hat{\mathbf{i}} + b_{\min} \cos(\theta) \hat{\mathbf{j}}$$

4. Negative Root Fillet Radius

$$R_{-RF} = (b_{\min} + rr_b) - \sqrt{rr_b^2 - L^2(\theta - \theta_{ini})^2}$$

$$1.9853 < \theta \leq 2.5294 \quad \theta_{ini} = 1.9853$$

$$\bar{\mathbf{P}} = R_{-RF} \cos(\theta) \hat{\mathbf{i}} + R_{-RF} \sin(\theta) \hat{\mathbf{j}}$$

$$\bar{\mathbf{T}} = \left\{ \frac{L^2(\theta - \theta_{ini}) \cos(\theta)}{\sqrt{rr_b^2 - L^2(\theta - \theta_{ini})^2}} - \left[(b_{\min} + rr_b) - \sqrt{rr_b^2 - L^2(\theta - \theta_{ini})^2} \right] \sin(\theta) \right\} \hat{\mathbf{i}}$$

$$\left\{ \frac{L^2(\theta - \theta_{ini}) \sin(\theta)}{\sqrt{rr_b^2 - L^2(\theta - \theta_{ini})^2}} + \left[(b_{\min} + rr_b) - \sqrt{rr_b^2 - L^2(\theta - \theta_{ini})^2} \right] \cos(\theta) \right\} \hat{\mathbf{j}}$$

5. Negative Flank Radius

$$R_{-F} = (b_{\max} + \frac{1}{2} rr_b) + K(\theta - \theta_{ini})$$

$$2.5294 < \theta \leq 4.2209 \quad \theta_{ini} = 2.5294$$

$$\bar{\mathbf{P}} = R_{-F} \cos(\theta) \hat{\mathbf{i}} + R_{-F} \sin(\theta) \hat{\mathbf{j}}$$

$$\bar{\mathbf{T}} = \left\{ K \cos(\theta) - \left[(b_{\min} + \frac{1}{2} rr_b) + K(\theta - \theta_{ini}) \right] \sin(\theta) \right\} \hat{\mathbf{i}}$$

$$\left\{ K \sin(\theta) + \left[(b_{\min} + \frac{1}{2} rr_b) + K(\theta - \theta_{ini}) \right] \cos(\theta) \right\} \hat{\mathbf{j}}$$

6. Negative Crest Fillet Radius

$$R_{-CF} = (b_{\max} - crr_b) + \sqrt{crr_b^2 - \left(\frac{\sqrt{3}}{2} crr_b - L(\theta - \theta_{ini}) \right)^2}$$

$$4.2209 < \theta \leq 4.4929 \quad \theta_{ini} = 4.2209$$

$$\bar{\mathbf{P}} = R_{-CF} \cos(\theta) \hat{\mathbf{i}} + R_{-CF} \sin(\theta) \hat{\mathbf{j}}$$

$$\bar{\mathbf{T}} = \left\{ \frac{L \left(\frac{\sqrt{3}}{2} crr_b - L(\theta - \theta_{ini}) \right) \cos(\theta)}{\sqrt{crr_b^2 - \left(\frac{\sqrt{3}}{2} crr_b - L(\theta - \theta_{ini}) \right)^2}} - \left[(b_{\max} - crr_b) + \sqrt{crr_b^2 - \left(\frac{\sqrt{3}}{2} crr_b - L(\theta - \theta_{ini}) \right)^2} \right] \sin(\theta) \right\} \hat{\mathbf{i}}$$

$$\left\{ \frac{L \left(\frac{\sqrt{3}}{2} crr_b - L(\theta - \theta_{ini}) \right) \sin(\theta)}{\sqrt{crr_b^2 - \left(\frac{\sqrt{3}}{2} crr_b - L(\theta - \theta_{ini}) \right)^2}} + \left[(b_{\max} - crr_b) + \sqrt{crr_b^2 - \left(\frac{\sqrt{3}}{2} crr_b - L(\theta - \theta_{ini}) \right)^2} \right] \cos(\theta) \right\} \hat{\mathbf{j}}$$

7. Crest Radius

$$R_C = b_{\max}$$

$$4.4929 < \theta \leq 4.9156 \quad \theta_{ini} = 4.4929$$

$$\vec{\mathbf{P}} = b_{\max} \cos(\theta) \hat{\mathbf{i}} + b_{\max} \sin(\theta) \hat{\mathbf{j}}$$

$$\vec{\mathbf{T}} = -b_{\max} \sin(\theta) \hat{\mathbf{i}} + b_{\max} \cos(\theta) \hat{\mathbf{j}}$$

8. Positive Crest Fillet Radius

$$R_{+CF} = (b_{\max} - crr_b) + \sqrt{crr_b^2 - L^2(\theta - \theta_{ini})^2}$$

$$4.9156 < \theta \leq 5.1877 \quad \theta_{ini} = 4.9156$$

$$\vec{\mathbf{P}} = R_{+CF} \cos(\theta) \hat{\mathbf{i}} + R_{+CF} \sin(\theta) \hat{\mathbf{j}}$$

$$\vec{\mathbf{T}} = \left\{ \frac{-L^2(\theta - \theta_{ini}) \cos(\theta)}{\sqrt{crr_b^2 - L^2(\theta - \theta_{ini})^2}} - \left[(b_{\max} - crr_b) + \sqrt{crr_b^2 - L^2(\theta - \theta_{ini})^2} \right] \sin(\theta) \right\} \hat{\mathbf{i}}$$

$$\left\{ \frac{-L^2(\theta - \theta_{ini}) \sin(\theta)}{\sqrt{crr_b^2 - L^2(\theta - \theta_{ini})^2}} + \left[(b_{\max} - crr_b) + \sqrt{crr_b^2 - L^2(\theta - \theta_{ini})^2} \right] \cos(\theta) \right\} \hat{\mathbf{j}}$$

9. Positive Flank Radius

$$R_{+F} = (b_{\max} - \frac{1}{2}crr_b) - K(\theta - \theta_{ini})$$

$$5.1877 < \theta \leq 6.2832 \quad \theta_{ini} = 5.1877$$

$$\vec{\mathbf{P}} = R_{+F} \cos(\theta) \hat{\mathbf{i}} + R_{+F} \sin(\theta) \hat{\mathbf{j}}$$

$$\vec{\mathbf{T}} = \left\{ -K \cos(\theta) - \left[(b_{\max} - \frac{1}{2}crr_b) - K(\theta - \theta_{ini}) \right] \sin(\theta) \right\} \hat{\mathbf{i}}$$

$$\left\{ -K \sin(\theta) + \left[(b_{\max} - \frac{1}{2}crr_b) - K(\theta - \theta_{ini}) \right] \cos(\theta) \right\} \hat{\mathbf{j}}$$

A.2 PARAMETRIC EQUATIONS – NUT

1. Negative Flank Radius

$$R_{-F} = (n_{\min} + \frac{1}{2}crr_n) + K(\theta + \theta_{ini})$$

$$0.0000 \leq \theta \leq 1.0520 \quad \theta_{ini} = 0.6394$$

$$\bar{\mathbf{P}} = R_{-F} \cos(\theta) \hat{\mathbf{i}} + R_{-F} \sin(\theta) \hat{\mathbf{j}}$$

$$\bar{\mathbf{T}} = \left\{ K \cos(\theta) - \left[(n_{\min} + \frac{1}{2}crr_n) + K(\theta + \theta_{ini}) \right] \sin(\theta) \right\} \hat{\mathbf{i}}$$

$$\left\{ K \sin(\theta) + \left[(n_{\min} + \frac{1}{2}crr_n) + K(\theta + \theta_{ini}) \right] \cos(\theta) \right\} \hat{\mathbf{j}}$$

2. Negative Root Fillet Radius

$$R_{-RF} = (n_{\max} - rr_n) + \sqrt{rr_n^2 - \left(\frac{\sqrt{3}}{2} rr_n - L(\theta - \theta_{ini}) \right)^2}$$

$$1.0520 < \theta \leq 1.3241 \quad \theta_{ini} = 1.0520$$

$$\bar{\mathbf{P}} = R_{-RF} \cos(\theta) \hat{\mathbf{i}} + R_{-RF} \sin(\theta) \hat{\mathbf{j}}$$

$$\bar{\mathbf{T}} = \left\{ \frac{L \left(\frac{\sqrt{3}}{2} rr_n - L(\theta - \theta_{ini}) \right) \cos(\theta)}{\sqrt{rr_n^2 - \left(\frac{\sqrt{3}}{2} rr_n - L(\theta - \theta_{ini}) \right)^2}} - \left[(n_{\max} - rr_n) + \sqrt{rr_n^2 - \left(\frac{\sqrt{3}}{2} rr_n - L(\theta - \theta_{ini}) \right)^2} \right] \sin(\theta) \right\} \hat{\mathbf{i}}$$

$$\left\{ \frac{L \left(\frac{\sqrt{3}}{2} rr_n - L(\theta - \theta_{ini}) \right) \sin(\theta)}{\sqrt{rr_n^2 - \left(\frac{\sqrt{3}}{2} rr_n - L(\theta - \theta_{ini}) \right)^2}} + \left[(n_{\max} - rr_n) + \sqrt{rr_n^2 - \left(\frac{\sqrt{3}}{2} rr_n - L(\theta - \theta_{ini}) \right)^2} \right] \cos(\theta) \right\} \hat{\mathbf{j}}$$

3. Root Radius

$$R_R = n_{\max}$$

$$1.3241 < \theta \leq 1.7467 \quad \theta_{ini} = 1.3241$$

$$\bar{\mathbf{P}} = n_{\max} \cos(\theta) \hat{\mathbf{i}} + n_{\max} \sin(\theta) \hat{\mathbf{j}}$$

$$\bar{\mathbf{T}} = -n_{\max} \sin(\theta) \hat{\mathbf{i}} + n_{\max} \cos(\theta) \hat{\mathbf{j}}$$

4. Positive Root Fillet Radius

$$R_{+RF} = (n_{\max} - rr_n) + \sqrt{rr_n^2 - L^2(\theta - \theta_{ini})^2}$$

$$1.7467 < \theta \leq 2.0188 \quad \theta_{ini} = 1.7467$$

$$\bar{\mathbf{P}} = R_{+RF} \cos(\theta) \hat{\mathbf{i}} + R_{+RF} \sin(\theta) \hat{\mathbf{j}}$$

$$\bar{\mathbf{T}} = \left\{ \frac{-L^2(\theta - \theta_{ini}) \cos(\theta)}{\sqrt{rr_n^2 - L^2(\theta - \theta_{ini})^2}} - \left[(n_{\max} - rr_n) + \sqrt{rr_n^2 - L^2(\theta - \theta_{ini})^2} \right] \sin(\theta) \right\} \hat{\mathbf{i}}$$

$$\left\{ \frac{-L^2(\theta - \theta_{ini}) \sin(\theta)}{\sqrt{rr_n^2 - L^2(\theta - \theta_{ini})^2}} + \left[(n_{\max} - rr_n) + \sqrt{rr_n^2 - L^2(\theta - \theta_{ini})^2} \right] \cos(\theta) \right\} \hat{\mathbf{j}}$$

5. Positive Flank Radius

$$R_{+F} = (n_{\max} - \frac{1}{2} rr_n) - K(\theta - \theta_{ini})$$

$$2.0188 < \theta \leq 3.7102 \quad \theta_{ini} = 2.0188$$

$$\bar{\mathbf{P}} = R_{+F} \cos(\theta) \hat{\mathbf{i}} + R_{+F} \sin(\theta) \hat{\mathbf{j}}$$

$$\bar{\mathbf{T}} = \left\{ -K \cos(\theta) - \left[(n_{\max} - \frac{1}{2} rr_n) - K(\theta - \theta_{ini}) \right] \sin(\theta) \right\} \hat{\mathbf{i}}$$

$$\left\{ -K \sin(\theta) + \left[(n_{\max} - \frac{1}{2} rr_n) - K(\theta - \theta_{ini}) \right] \cos(\theta) \right\} \hat{\mathbf{j}}$$

6. Positive Crest Fillet Radius

$$R_{+CF} = (n_{\min} + crr_n) - \sqrt{crr_n^2 - \left(\frac{\sqrt{3}}{2} crr_n - L(\theta - \theta_{ini}) \right)^2}$$

$$3.7102 < \theta \leq 4.2543 \quad \theta_{ini} = 3.7102$$

$$\bar{\mathbf{P}} = R_{+CF} \cos(\theta) \hat{\mathbf{i}} + R_{+CF} \sin(\theta) \hat{\mathbf{j}}$$

$$\bar{\mathbf{T}} = \left\{ \frac{-L \left(\frac{\sqrt{3}}{2} crr_n - L(\theta - \theta_{ini}) \right) \cos(\theta)}{\sqrt{crr_n^2 - \left(\frac{\sqrt{3}}{2} crr_n - L(\theta - \theta_{ini}) \right)^2}} - \left[(n_{\min} + crr_n) - \sqrt{crr_n^2 - \left(\frac{\sqrt{3}}{2} crr_n - L(\theta - \theta_{ini}) \right)^2} \right] \sin(\theta) \right\} \hat{\mathbf{i}}$$

$$\left\{ \frac{-L \left(\frac{\sqrt{3}}{2} crr_n - L(\theta - \theta_{ini}) \right) \sin(\theta)}{\sqrt{crr_n^2 - \left(\frac{\sqrt{3}}{2} crr_n - L(\theta - \theta_{ini}) \right)^2}} + \left[(n_{\min} + crr_n) - \sqrt{crr_n^2 - \left(\frac{\sqrt{3}}{2} crr_n - L(\theta - \theta_{ini}) \right)^2} \right] \cos(\theta) \right\} \hat{\mathbf{j}}$$

7. Crest Radius

$$R_C = n_{\min}$$

$$4.2543 < \theta \leq 5.0996 \quad \theta_{ini} = 4.2543$$

$$\vec{\mathbf{P}} = n_{\min} \cos(\theta) \hat{\mathbf{i}} + n_{\min} \sin(\theta) \hat{\mathbf{j}}$$

$$\vec{\mathbf{T}} = -n_{\min} \sin(\theta) \hat{\mathbf{i}} + n_{\min} \cos(\theta) \hat{\mathbf{j}}$$

8. Negative Crest Fillet Radius

$$R_{-CF} = (n_{\min} - crr_n) - \sqrt{crr_n^2 - L^2(\theta - \theta_{ini})^2}$$

$$5.0996 < \theta \leq 5.6438 \quad \theta_{ini} = 5.0996$$

$$\vec{\mathbf{P}} = R_{-CF} \cos(\theta) \hat{\mathbf{i}} + R_{-CF} \sin(\theta) \hat{\mathbf{j}}$$

$$\vec{\mathbf{T}} = \left\{ \frac{L^2(\theta - \theta_{ini}) \cos(\theta)}{\sqrt{crr_n^2 - L^2(\theta - \theta_{ini})^2}} - \left[(n_{\min} + crr_n) - \sqrt{crr_n^2 - L^2(\theta - \theta_{ini})^2} \right] \sin(\theta) \right\} \hat{\mathbf{i}}$$

$$\left\{ \frac{L^2(\theta - \theta_{ini}) \sin(\theta)}{\sqrt{crr_n^2 - L^2(\theta - \theta_{ini})^2}} + \left[(n_{\min} + crr_n) - \sqrt{crr_n^2 - L^2(\theta - \theta_{ini})^2} \right] \cos(\theta) \right\} \hat{\mathbf{j}}$$

9. Negative Flank Radius

$$R_{-F} = (n_{\min} + \frac{1}{2}crr_n) + K(\theta - \theta_{ini})$$

$$5.6438 < \theta \leq 6.2832 \quad \theta_{ini} = 5.6438$$

$$\vec{\mathbf{P}} = R_{-F} \cos(\theta) \hat{\mathbf{i}} + R_{-F} \sin(\theta) \hat{\mathbf{j}}$$

$$\vec{\mathbf{T}} = \left\{ K \cos(\theta) - \left[(n_{\min} + \frac{1}{2}crr_n) + K(\theta - \theta_{ini}) \right] \sin(\theta) \right\} \hat{\mathbf{i}}$$

$$\left\{ K \sin(\theta) + \left[(n_{\min} + \frac{1}{2}crr_n) + K(\theta - \theta_{ini}) \right] \cos(\theta) \right\} \hat{\mathbf{j}}$$

APPENDIX B

B.1 Contact Pair Line Segment Endpoints

When a contact occurs between the bolt and nut, there will be a list of contact pairs returned by RAPID, which are defined as one triangle each of the bolt and nut. The determination of the line segment created by this intersection is required to isolate the contact point location. Four types of contact pairs have the potential to occur:

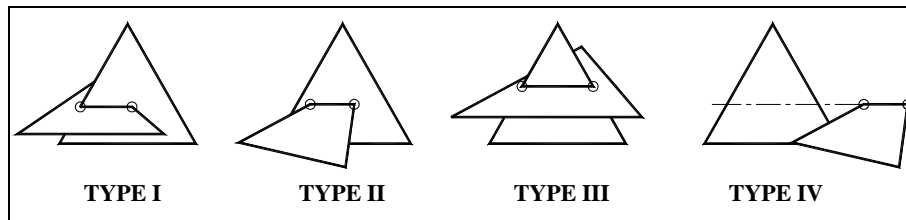


Figure B.1. 1

The ordered pairs of points, which define the endpoints of the line segment, are listed in a table for each type of contact pair. For more information, please reference chapter 3 section 3.6.

TYPE I

	θ_0^1	θ_0^2	θ_1^1	θ_1^2
$(n_{c2}, b_{c1}, n_{c3}, b_{c2})$	π	0	0	0
$(n_{c3}, b_{c1}, n_{c2}, b_{c2})$	0	π	0	0
$(n_{c2}, b_{c2}, n_{c3}, b_{c1})$	0	0	π	0
$(n_{c3}, b_{c2}, n_{c2}, b_{c1})$	0	0	0	π

Table B.1. 1

TYPE II

	θ_0^1	θ_0^2	θ_1^1	θ_1^2
$(b_{c1}, n_{c2}, n_{c3}, b_{c2})$	0	0	0	0
$(b_{c2}, n_{c2}, n_{c3}, b_{c1})$	0	0	0	0
$(b_{c2}, n_{c3}, n_{c2}, b_{c1})$	0	0	0	0
$(b_{c1}, n_{c3}, n_{c2}, b_{c2})$	0	0	0	0

Table B.1. 2

TYPE III

	θ_0^1	θ_0^2	θ_1^1	θ_1^2
$(n_{c2}, b_{c1}, b_{c2}, n_{c3})$	π	0	π	0
$(n_{c2}, b_{c2}, b_{c1}, n_{c3})$	0	π	0	π
$(n_{c3}, b_{c2}, b_{c1}, n_{c2})$	0	π	0	π
$(n_{c3}, b_{c1}, b_{c2}, n_{c2})$	π	0	π	0

Table B.1. 3**TYPE IV**

	θ_0^1	θ_0^2	θ_1^1	θ_1^2
$(n_{c2}, n_{c3}, b_{c1}, b_{c2})$	π	0	0	π
$(n_{c2}, n_{c3}, b_{c2}, b_{c1})$	π	0	0	π
$(n_{c3}, n_{c2}, b_{c2}, b_{c1})$	0	π	π	0
$(n_{c3}, n_{c2}, b_{c1}, b_{c2})$	0	π	π	0

Table B.1. 4

APPENDIX C

C.1 Pivot Direction Algorithm

After the bolt obtains the second contact, it will pivot about an axis defined by the two contact points. The direction of rotation is influenced by several factors defined as:

- The quadrant location of CP_0 and CP_1
- Where the X_P -axis intersects the X_F -axis (positive or negative)
- The slope of the X_P -axis (positive or negative).

All of these parameters are measured with respect to the fixed reference frame. The entire set of possibilities are shown below:

CP_0	X_P axis intersects	Slope	CP_1	DIR of ROT
Q1	$+X_F$	Negative	Q2	Negative
			Q4	Positive
		Positive	Q3	Positive
			Q4	Positive
	$-X_F$	Negative	IMP	
		Positive	Q2	Negative
			Q3	Negative

Table C.1. 1

CP_0	X_P axis intersects	Slope	CP_1	DIR of ROT
Q2	$+X_F$	Negative	Q1	Positive
			Q4	Positive
		Positive	IMP	
	$-X_F$	Negative	Q3	Negative
			Q4	Negative
		Positive	Q1	Positive
			Q2 & Q3	Negative

Table C.1. 2

CP₀	X_P axis intersects	Slope	CP₁	DIR of ROT
Q3	+X _F	Negative	IMP	
		Positive	Q1	Negative
			Q4	Negative
	-X _F	Negative	Q2	Positive
			Q3 & Q4	Negative
		Positive	Q1	Positive
			Q2	Positive

Table C.1. 3

CP₀	X_P axis intersects	Slope	CP₁	DIR of ROT
Q4	+X _F	Negative	Q1	Negative
			Q2	Negative
		Positive	Q1	Negative
			Q3 & Q4	Positive
	-X _F	Negative	Q2	Positive
			Q3	Positive
		Positive	IMP	

Table C.1. 4

APPENDIX D

D.1 RAPID Collision Detection Library Commands

Each facet of a tessellated surface is read from the binary (STL) file and stored in a RAPID model. RAPID accepts only one complete facet per loop iteration; therefore, one execution of the input command consists of three vertices and an identification number. The identification number is the only way one can keep track of its position in space, and it is used extensively in the program to extract vertex information from memory. The following defines the entire set of *Rapid* commands utilized in the program:

RAPID_model * <i>model name</i>	defines the name of the model
<i>model name</i> →BeginModel()	informs <i>Rapid</i> library that facets will be stored.
<i>model name</i> →AddTri(p0, p1, p2, id)	adds three vertices to the library labeled p0, p1, and p2 along with the facets identification number.
<i>model name</i> →EndModel()	informs the library that facet input is complete
RAPID_Collide(R1, T1, 1 st <i>model name</i> , R2, T2, 2 nd <i>model name</i> , <i>contact command</i>)	This command calls the contact detection algorithm in the <i>Rapid</i> library with the model name, the rotation matrix, R, and translation vector, T, for the both models. The <i>contact command</i> has two settings shown below.
RAPID_FIRST_CONTACT	This <i>contact command</i> instructs the library to return just the first facet it detects.
RAPID_ALL_CONTACTS	This <i>contact command</i> instructs the library to return all the facets in contact.
RAPID_num_contacts	This variable from the library contains the total number of contact pairs.
RAPID_contact[<i>contact #</i>].id#	This command extracts the facet id number associated with the contact number, where the <i>contact #</i> ranges from zero to RAPID_num_contacts (or total number of contact pairs). The id# identifies which model number to parse. For model #1, the id number would be id1.

RAPID only provides the facet identification numbers when returning a contact pair. The vertices of the triangles in contact are then retrieved from the multi-dimensional

permanent storage array. The first column of this array contains the identification number, while the next nine contain the X, Y, and Z coordinates of the three vertices. For further information about collision detection libraries as well as a full instruction manual, the reader is encouraged to contact the following web site:

http://www.cs.unc.edu/~geom/collide_packages.html

D.2 Collision Detection Program of a #1/4-20 UNC Assembly

This section provides the code that calculates multiple contact points and the respective common normals during the initial phase of a #1/4-20 UNC threaded assembly. For more information concerning the program structure, please reference the comments throughout the code.